

PROGRESS AT THE JEFFERSON LABORATORY FEL*

C. Tennant[#], Jefferson Laboratory, Newport News, VA 23606, U.S.A.

Abstract

As the only currently operating free electron laser (FEL) based on a CW superconducting energy recovering linac (ERL), the Jefferson Laboratory FEL Upgrade remains unique as an FEL driver. The present system represents the culmination of years of effort in the areas of SRF technology, ERL operation, lattice design, high power optics and DC photocathode gun technology. In 2001 the FEL Demo generated 2.1 kW of laser power. Following extensive upgrades, in 2006 the FEL Upgrade generated 14.3 kW of laser power breaking the previous world record. The FEL Upgrade remains a valuable testbed for studying a variety of collective effects, such as the beam breakup instability, longitudinal space charge and coherent synchrotron radiation. Additionally, there has been exploration of operation with lower injection energy and higher bunch charge. Recent progress and achievements in these areas will be presented, and two recent milestones – installation of a UV FEL and establishment of a DC gun test stand – will be discussed. Additionally, a review of the longitudinal matching scheme and the use of incomplete energy and its implications will be presented.

INTRODUCTION

Jefferson Laboratory has over a decade of operational experience with high power ERL-based drivers for FELs. In the following sections we provide a synopsis of some of the primary challenges for achieving maximum accelerator, and hence FEL, performance. Following a brief description of the IR FEL Demo and the currently operating FEL Upgrade, we give an overview of the various collective effects that one expects when dealing with an intense beam of electrons and how they are managed in the FEL Upgrade Driver. Examples include the beam breakup (BBU) instability, space charge and coherent synchrotron radiation (CSR). We then discuss other important - and perhaps not fully appreciated - issues that can affect the performance of ERL-driven FELs. In particular, an overview of the longitudinal matching scheme to manage the large energy spread (imposed on the electron beam during lasing) is presented. It is then shown that for a system which lases strongly, the need arises to operate with incomplete energy recovery. This, in turn, has important ramifications for the linac RF drive system which are explored. A discussion of magnetic field quality and implications for ERL system performance is also presented. Finally, some recent results of transverse phase space tomography are reported.

JEFFERSON LAB FEL: PAST

Even before the Continuous Electron Beam Accelerator Facility (CEBAF) was completed, proposals were made for using an SRF linac as a driver for an FEL [1]. In addition to the ability of an SRF linac to maintain superior beam quality, the ability for CW operation opened up the possibility of achieving high average output power while using bunches of modest charge. It had been recognized that invoking energy recovery would increase the system efficiency while at the same time reducing the need for expensive, high power RF sources [2]. An initial design for an ERL-based driver for an FEL at Jefferson Laboratory was developed in 1991 [3]. This design was significant in that it marked the first time energy recovery was implemented as the nominal mode of operation. By 1998 the Jefferson Laboratory IR FEL Demo successfully energy recovered 5 mA of average beam current through a single cryomodule from 48 MeV to the injection energy of 10 MeV [4]. Before its decommissioning in 2001, the IR Demo FEL had established a new world record for average laser power at 2.1 kW (besting the previous record of 11 W).

JEFFERSON LAB FEL: PRESENT

The current Jefferson Laboratory FEL is an upgrade to the IR FEL Demo. Regarding the accelerator, the most substantial upgrades are an additional two cryomodules to increase the beam energy to 115 MeV and doubling the injected current from 5 mA to 10 mA. The FEL Upgrade started commissioning in 2003, achieved first light in 2003 and in October of 2006 generated 14.3 kW of laser power at 1.6 μm [5].

A schematic of the FEL Upgrade is shown in Fig. 1. Electrons are generated in a DC photocathode gun, accelerated to 9 MeV and injected into the linac where they are further accelerated up to 115 MeV through three cryomodules (each containing 8 superconducting radio frequency (SRF) niobium cavities). The beam is transported to a wiggler. Because the SRF linac supports continuous wave (CW) beam, high average laser power can be achieved with a high bunch repetition rate and only modest single bunch charge (135 pC). The spent electron beam is recirculated and phased in such a way that the beam is decelerated through the linac on the second pass. Upon exiting the linac, the energy recovered beam is extracted to a dump.

*Work supported by the Office of Naval Research, the Joint Technology Office, the Commonwealth of Virginia, the Air Force Research Laboratory, and by the DOE Contract DEAC05-84ER40150

[#]tennant@jlab.org

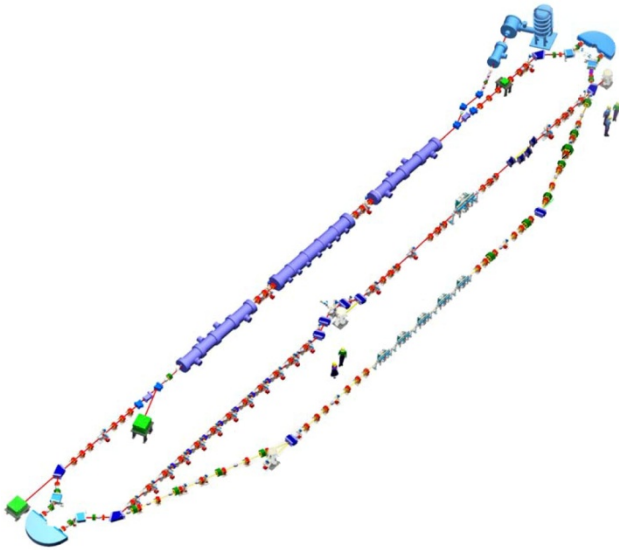


Figure 1: A schematic of the Jefferson Laboratory FEL Upgrade showing both the IR and UV FEL beamlines.

Hardware Upgrades and Additions

In the last two years, we have seen the addition of a separate (nearly complete) UV FEL beamline (refer to Fig. 1) and a gun test stand (GTS). When commissioned, the new FEL beamline is expected to generate several 10s of Watts in the UV. The beamline is also designed to allow the option for testing an amplifier-type FEL [6]. Such an experiment would be significant as it would provide a way to directly compare oscillator and amplifier FEL performance. The purpose of the GTS is to test gun high voltage performance with coated electrodes for field emission suppression, provide dedicated operations for electron beam characterization at high charge and to have the ability to characterize photocathode lifetime with improved methods and materials for better vacuum conditions [7].

Collective effects

The FEL Upgrade Driver has successfully managed all the well documented collective effects that one expects in an ERL-based FEL driver [8]. These include the limit of high average beam current due to beam breakup, the phase space dilution from the space charge force and the deleterious phase space distortion due to short bunch lengths from CSR. A few comments on each are given below:

BBU

In 2005 the threshold current for beam breakup decreased significantly, due to the installation of a cryomodule with inadequately damped higher-order modes (HOMs), and the instability was observed. A thorough suite of measurements were performed which characterized the instability and successfully benchmarked data with existing simulation codes [9,10,11]. Using this information, and through clever beam optical suppression techniques, BBU is no longer an

operational impediment. For high average current operations, the FEL Upgrade Driver utilizes five skew-quadrupoles to interchange the horizontal and vertical phase spaces thereby effectively breaking the feedback loop between the beam and the HOM causing BBU [12]. Fundamentally, the instability is a result of inadequately damped cavity HOMs. To address this issue, Jefferson Laboratory has designed and performed RF measurements of a new, strongly damped cavity. Simulations of this cavity in a novel ERL-based FEL designed for Florida State University give threshold currents on the order of 1 A [13].

Space Charge

At the nominal 135 pC transverse space charge does not present any problems, however, longitudinal space charge (LSC) can adversely affect machine performance at this bunch charge if not properly handled. The initial indication of LSC in the Upgrade driver was the observation of energy spread asymmetry about the linac on-crest phase [14]. Figure 2 displays streak camera measurements showing the longitudinal phase space for several off-crest acceleration phases [15].

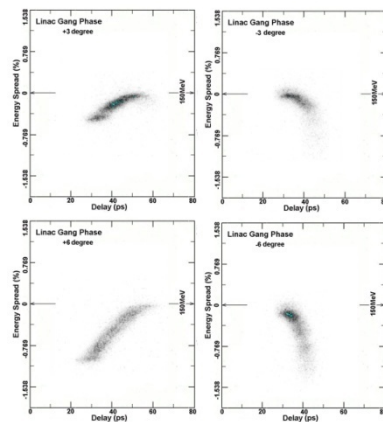


Figure 2: Streak camera measurements showing the longitudinal phase space as a function of off-crest acceleration phase. The two measurements on the left (right) correspond to accelerating on the rising (falling) part of the RF waveform. The two top (bottom) measurements are for an off-crest phase of 3° (6°).

There are several interesting features to consider. First, note that for bunches accelerated on the falling part of the RF waveform, the bunch is shorter than for accelerating on the rising part of the waveform. This is due to the positive M_{56} from the exit of the linac to the location of the measurement (the midpoint of the 180° bend in the first Bates bend) [16]. The second, and more interesting, feature to notice is the increased energy spread when accelerating on the falling part of the waveform due to the LSC wake. That is, the high energy head gains energy while the low energy tail loses energy. Operating on the rising part of the waveform leads to a decrease in the energy spread as the low energy head gains energy and the high energy tail loses energy (see the schematic in Fig.

3 illustrating the effect). These measurements were made using a modest bunch charge of 110 pC and the effects of LSC are clearly seen, becoming more pronounced the closer the bunch sits to crest. To avoid longitudinal emittance dilution at the wiggler, we accelerate on the rising part of the RF waveform to minimize the deleterious effects of LSC.

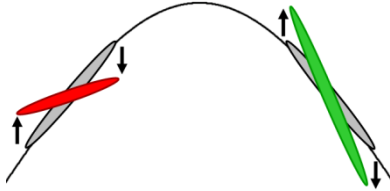


Figure 3: Schematic showing the effect of LSC on a bunch accelerated before and after crest.

CSR

Although we observe the effects of CSR, it has not proved to be a hindrance for beam operations. In fact, CSR is used as a diagnostic to tune up the machine. When CSR begins to “turn on”, then we know that the bunch length is properly compressed for the FEL. We have performed initial beam based measurements to characterize CSR; however the difficulty of studying this effect in the FEL Upgrade is the complexity of the longitudinal phase space. For instance, in the first Bates bend the bunch goes through two parasitic compressions – all before the final compression at the wiggler entrance. We also observe filamentation of the beam as it becomes strongly compressed (see Fig. 4). The challenge is distinguishing the contributions from LSC, CSR and other wakes to these observations. Efforts are being made to more accurately simulate CSR in the FEL.

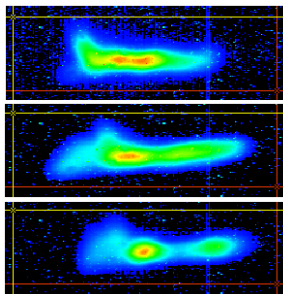


Figure 4: Images from a synchrotron light monitor showing beam filamentation as a function of bunch length compression (courtesy P. Evtunshenko).

Longitudinal Match and Incomplete ER

Reduced to its primary objective, the Upgrade Driver must generate a short bunch (high peak current) at the wiggler and energy compress and energy recover the large longitudinal phase space of the spent electron beam following the wiggler. The injector is designed to generate a long bunch with low momentum spread. The objective of the Driver is to rotate the longitudinal phase space 90° to create a short bunch at the wiggler. Following the

wiggler, the longitudinal phase space must be rotated back by 90° to energy compress the beam which has acquired a large energy spread. These longitudinal phase space manipulations are achieved by accelerating off-crest through the linac to impart a phase-energy correlation. Rotation of the phase space to an upright ellipse at the wiggler is accomplished with a proper management of the momentum compactions (both first- and second-order) in the first 180° bend and in a downstream magnetic chicane. Similar longitudinal phase space manipulations are used to properly manage the beam after the wiggler to the beam dump. Due to the large energy spread, multipole correction through third-order is required [17,18].

As a consequence of the large energy spread, care must be taken to ensure that the entire bunch precedes the trough of the RF waveform during energy recovery. Failure to do so leads to an unmanageable high energy tail after deceleration. To first-order, to prevent the beam from falling into the trough of the RF waveform, the deceleration phase must exceed

$$\phi_o = \cos^{-1} \left(1 - \frac{1}{2} \frac{\Delta E}{E} \right) \quad (1)$$

where we take the fractional energy spread to be approximately 6 times the FEL extraction efficiency. Thus for 2% extraction efficiency it is required to operate with the bunch centroid 20° before trough.

By shifting the bunch further up the waveform to accommodate the full energy spread, the beam central energy is no longer at a phase that is 180° from the accelerating beam, a condition referred to as incomplete energy recovery. If one tries to restore the condition of perfect energy recovery by accelerating further off-crest, the resulting energy spread will exceed the wiggler’s acceptance. In an effort to avoid this one might consider injecting a shorter bunch; however this results in phase space dilution due to LSC. In short, the longitudinal operating point lives in a highly constrained parameter space and a number of trade-offs must be considered.

RF Transients

In addition to the increasing the energy spread, lasing also leads to a decrease of the central energy of the bunch as energy is transferred from the electron beam to the optical beam. The lower energy bunches couple with the nonzero momentum compaction (M_{56}) of the recirculator lattice to generate a change in the path length (or equivalently, a phase shift). Thus the RF system must deal with a phase shift of several degrees as the laser turns on and off. Because the phase shifts occur on the timescale of the laser turn on/off, even piezo-tuners cannot tune the cavities fast enough. During this time sufficient RF power must be delivered to maintain the gradient in the cavities at a level consistent with the available energy aperture of the machine. The absence of sufficient RF overhead will lead to beam loss and an eventual machine trip [19].

There also exists an RF transient for initial beam turn on when the machine is configured for incomplete energy recovery. Figure 5 show the agreement between an

analytic model and measurements at the FEL Upgrade of the klystron power during beam turn on. In this measurement the data was taken under two sets of conditions: (1) the cavity tuner was allowed to operate and correct for the off-crest beam loading as the beam current was increased from 0 to 4.25 mA (2) the tuner was allowed to tune the cavity only when beam was off. The data was recorded from a Jefferson Laboratory 7-cell cavity with a Q_L of 2×10^7 and was operated at 5.6 MV/m. (Note that the forward power signal was not well calibrated and so these figures are provided only to demonstrate the effect rather than to quantify it).

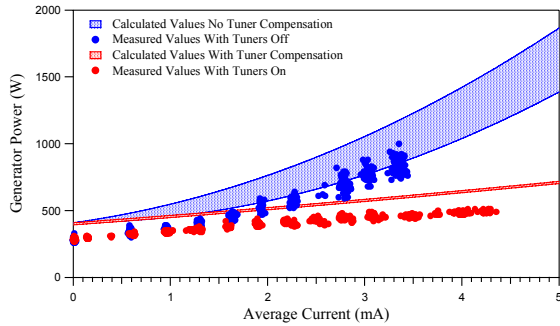


Figure 5: Measured data showing generator power as a function of beam current with the cavity tuners on to compensate for the reactive power (red) and off (blue).

Dynamic loading due to incomplete energy recovery is an issue for all accelerators that use energy recovery. In some machines it is due to unintentional errors imposed on the energy recovered beam; for instance, path length errors in large-scale light sources. In other machines, such as high power ERL-based FEL drivers, it is done intentionally. In cases where there is the potential for rapid changes in the relative phase of the energy recovered beam, dynamic loading would be difficult to completely control using fast tuners. In such cases adequate headroom in the RF power will have to be designed into the system.

Magnetic Field Quality

An often overlooked aspect of ERL design, and one with significant implications for system performance, is magnetic field quality. Poor field quality leads to transverse steering errors, which due to the non-zero M_{52} of the recirculator leads to path length errors (or equivalently, phase shifts). Such phase shifts, in turn, increase the energy spread of the bunch and can lead to an unmanageably large energy spread at the dump [20].

For an error field of ΔB over a length l , the phase offset of a bunch (relative to the nominal RF phase) is given by

$$\delta\phi = \left(\frac{2\pi M_{52}}{\lambda_{RF}}\right) \left(\frac{\Delta B l}{B\rho}\right) \quad (2)$$

where λ_{RF} is the wavelength of the RF fundamental frequency and $B\rho$ is the beam rigidity. For a linac with energy gain, E_L , the energy recovered during deceleration

at the nominal RF phase ϕ_o is $E = E_L \cos(\phi_o)$. It follows that the energy shift generated from a phase error, $\delta\phi$ is given by

$$\Delta E = E_L [\cos(\phi_o + \delta\phi) - \cos(\phi_o)] \cong -E_L \sin(\phi_o) \delta\phi \quad (3)$$

An estimate of the final energy spread after energy recovery as it relates to the relative field error, $\Delta B/B$, is found by inserting Eq. (2) into Eq. (3)

$$\Delta E = -\left(\frac{2\pi M_{52}}{\lambda_{RF}}\right) E_L \sin \phi_o \left(\frac{\Delta B}{B}\right) \theta \quad (4)$$

where θ is the total bend angle. Note well that for a fixed final energy spread, the relative field error must decrease as the linac energy gain increases. As an example, for the FEL Upgrade operating at 115 MeV, 20° off-crest and with an average M_{52} of 1 m, the absolute energy spread at the dump is 0.1 MeV and the total bend angle (from wiggler to dump) through the Bates bend is 352° . This leads to a relative field error tolerance of 1.3×10^{-5} which is a factor of ~ 7 below the 10^{-4} specified (and achieved) for the dipoles (see Fig. 6) [21]. However with the large energy acceptance of the dump beamline in addition to the multipole correction (through third-order) in the recirculation arc, this becomes manageable [22].

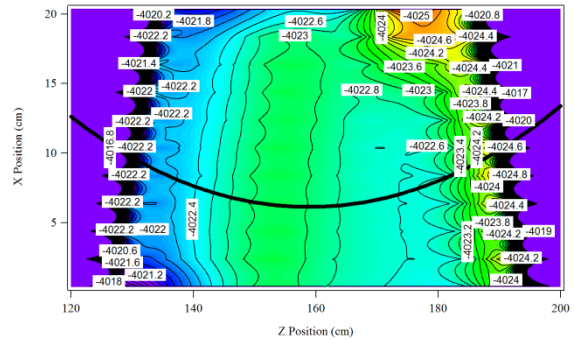


Figure 6: Measured data of a dipole before installation in the Upgrade driver exhibiting 1 part in 10,000 field homogeneity at 145 MeV. The thick black trace represents the beam trajectory.

Phase Space Tomography

Phase space tomography is a powerful tool which allows one to reconstruct a beam phase space (x, x' or y, y') that is not captured by conventional beam diagnostics. Initial transverse phase space tomography measurements were made at the FEL Upgrade recently [23]. An example is displayed in Fig. 7. Measurements were made in the backleg region of the FEL Upgrade which is comprised of six 90° FODO cells. Ideally the rotation of the phase space would span 180° . In the measurement we generated a rotation of 0.87π . For reconstruction algorithms such as filtered backprojection, this would be an insufficient measurement and lead to severe artifacts in the reconstructed phase space. By using a robust iterative algorithm such as Maximum Entropy such artifacts are minimized [24,25]. Another important feature,

particularly for accelerator applications, is that even a limited number of measurements (which does not span a full 180°) produce very good results. As a way to test the validity of the measurements we note that the extracted emittance agrees to within 2% of a measurement of the emittance (in a region upstream) done via a quadrupole scan that same day. Furthermore, the extracted Twiss parameters at this location are consistent with the values expected from a perfectly match FODO cell.

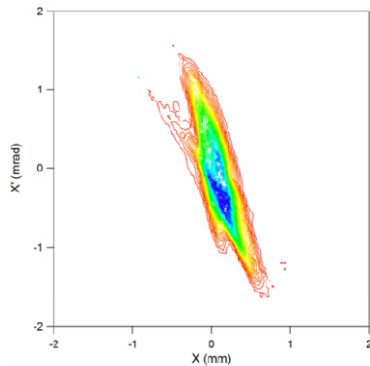


Figure 7: Reconstructed transverse phase space, represented as a contour plot, from the FEL Upgrade driver.

JEFFERSON LAB FEL: FUTURE

In the future Jefferson Laboratory expects to play an active role in the development of a 4th generation light source by leveraging experience and expertise in:

DC photocathode guns

The DC photocathode gun for the FEL has consistently and reliably performed at a high level, generating up to 9 mA of average beam current. And now with a dedicated gun test facility, studies to advance the frontiers of this gun technology can continue.

Superconducting RF

Jefferson Laboratory is the only producer of SRF accelerators from top-to-bottom; from the physics requirements to fully commissioned hardware. Furthermore, Jefferson Laboratory has processed over half of the world's SRF cavities and the vast majority of CW cavities. At CEBAF alone we have over 50 cavity-centuries of operating experience.

Electron Beam Transport Design

The electron beam transport system has handled in excess of 1 MW recirculating beam power, while controlling collective effects, maintaining beam brightness, effectively managing longitudinal phase space and providing large acceptance transport to the beam dump. The lattice design of the FEL Upgrade has also proven to be remarkably robust. In addition to handling the beam dynamics challenges outlined above, the FEL driver has explored new regions of operational parameter space. For instance, we have established an operational configuration with an injection energy as low as 5 MeV

while concurrently pushing the charge per bunch to 270 pC [6]. In another test of the robustness of the transport system, the machine was configured for three pass operation where the first pass beam accelerated, second pass beam coasted and third pass beam decelerated through the linac [26].

ERL machine operation

In addition to 15 years of operating the recirculating accelerator CEBAF, Jefferson Laboratory has successfully demonstrated same-cell energy recovery in four different accelerators [4][5][27][28].

ACKNOWLEDGEMENTS

The author would like to thank the Jefferson Laboratory FEL Team for their fruitful discussions and assistance in assembling this material.

REFERENCES

- [1] G. Krafft and J. Bisognano, *Proc. PAC*, p. 1256 (1989).
- [2] R. Rohatgi, H. Schwettman, and T. Smith, *Proc. PAC*, p. 230 (1987).
- [3] D. Douglas et al., JLAB-TN 91-017 (1991).
- [4] G. Neil et al., PRL Vol. 84, No 4 (2000).
- [5] S. Benson et al., *Proc. PAC*, p. 79, (2007).
- [6] K. Jordan et al., in *Proc. PAC*, p. 1329, (2007).
- [7] C. Hernandez-Garcia, talk PESP Workshop (2008).
- [8] L. Merminga, *Proc. EPAC*, p. 16 (2004).
- [9] C. Tennant et al., *Phys. Rev. ST-AB* **8**, 074403 (2005).
- [10] D. Douglas et al., *Phys. Rev. ST-AB* **9**, 064403 (2006).
- [11] C. Tennant, Ph.D. thesis, The College of William and Mary (2006).
- [12] R. Rand and T. Smith, *Part. Accel.* **11**, 1 (1980).
- [13] F. Marhauser et al., *Proc. EPAC*, p. 886 (2008).
- [14] C. Hernandez-Garcia et al., *Proc. FEL Conf.*, p. 363 (2004).
- [15] S. Zhang et al., *Proc. FEL Conf.*, p. 740 (2006).
- [16] D. Douglas, *private communication*.
- [17] D. Douglas et al., JLAB-TN 95-015 (1995).
- [18] P. Piot, D. Douglas, and G. Krafft, *Phys. Rev. ST-AB* **6**, 030702 (2003).
- [19] T. Powers and C. Tennant, *Proc. ERL Workshop*, p. 75 (2007).
- [20] D. Douglas, JLAB-TN 02-002 (2002).
- [21] T. Hiatt et al., *Proc. PAC*, p. 2189 (2003).
- [22] J. Flanz and C. Sargent, *Proc. PAC*, p. 3213 (1985).
- [23] C. Tennant and Y. Roblin, JLAB-TN 09-021 (2009).
- [24] G. Minerbo, *Computer Graphics and Image Proc.* **10**, p. 46 (1979).
- [25] J. Scheins, TESLA Report 2004-08 (2004).
- [26] D. Douglas FEL FLOG 1167311 (2003).
- [27] N. Sereno et al., *Proc. PAC*, p. 3246 (1993).
- [28] C. Tennant et al., *Proc. SRF Workshop* (2003).